Published in final edited form as:
Small. 2014 February 26; 10(4): 812–819. doi:10.1002/smll.201301998.

In vivo immune cell distribution of gold nanoparticles in naïve and tumor bearing mice

Joao Paulo Mattos Almeida[†,⊥], **Adam Yuh Lin**[†,⊥], **Robert James Langsner**[†], **Phillip Eckels**[#], **Aaron Edward Foster**[‡,#], and **Rebekah Anna Drezek**[†,*]

[†]Department of Bioengineering, Rice University, Houston, Texas, USA.

[‡]Center for Cell and Gene Therapy, Baylor College of Medicine, Houston, Texas, USA.

[#]Bellicum Pharmaceuticals, Houston, Texas, USA.

Abstract

Gold nanoparticles (AuNPs) have been widely used for drug delivery and have recently been explored for applications in cancer immunotherapy. Although AuNPs are known to accumulate heavily in the spleen, the particle distribution within immune cells has not been thoroughly studied. Here, we characterize the cellular distribution of Cy5 labeled 50 nm AuNPs within the immune populations of the spleen from naïve and tumor bearing mice using flow cytometry. Surprisingly, approximately 30% of the detected AuNPs were taken up by B cells at 24 hours, with about 10% in granulocytes, 18% in dendritic cells, and 8% in T cells. In addition, 3% of the particles were detected within myeloid derived suppressor cells, an immune suppressive population that could be targeted for cancer immunotherapy. Furthermore, we observed that, over time, the particles traveled from the red pulp and marginal zone to the follicles of the spleen. Taking into consideration that the particle cellular distribution did not change at 1, 6 and 24 hours, it is highly suggestive that the immune populations carry the particles and migrate through the spleen instead of the particles migrating through the tissue by cell-cell transfer. Finally, we observed no difference in particle distribution between naïve and tumor bearing mice in the spleen and detected nanoparticles within 0.7% of dendritic cells of the tumor microenvironment. Overall, these results can help inform and influence future AuNP delivery design criteria including future applications for nanoparticle-mediated immunotherapy.

Keywords

Gold nanoparticles; Immunotherapy; Biodistribution; Immune system; Cancer; Spleen

[*]Author for correspondence: drezek@rice.edu.
[⊥]Authors contributed equally.

Supplementary information available

Particle characterization data, percentage of marker^{+}Cy5^{+} data in the spleen, and histology of spleens treated with AuNPs coated with unlabeled PEG. This material is available from the Wiley Online Library or from the authors.

1. Introduction

Gold nanoparticles (AuNPs) have been applied in a number of cancer treatment modalities including drug delivery, gene therapy, and photothermal ablation.[1–4] AuNPs can be easily synthesized and can be modified with a variety of materials including drugs,[2] polymers,[5] targeting ligands,[6] and nucleic acids.[7] Recently, AuNPs have been used for cancer immunotherapy as delivery vehicles for cancer antigens and immune adjuvants.[8, 9] Gold nanoparticles are well suited for immune cell targeting, for they are naturally taken up by the immune system upon *in vivo* injection, and it has been shown that AuNP mediated delivery enhances the effect of tumor antigens[8, 10, 11] and immune adjuvants.[9, 12]

Yet, despite numerous studies focused on the biodistribution of gold nanoparticles, very little has been done to understand the cellular level distribution of nanoparticles *in vivo*, particularly within cells of the immune system. Biodistribution studies have focused on gold accumulation at the organ level, demonstrating that AuNPs show the highest accumulation in the liver and spleen.[13–16] Shah et al. observed that gold nanoparticles traversed from the red pulp to the white pulp of the spleen over time but did not identify the immune cells involved in particle uptake.[17] In the liver, Bartneck and colleagues observed 30 fold higher accumulation of gold nanorods in immature macrophages as opposed to Kupffer cells; given that immature macrophages can cause inflammatory liver injury, their finding emphasizes the importance of identifying immune cell subsets that take up nanoparticles.[18] Therefore, in this study, we sought to characterize the distribution of gold nanoparticles within the major immune populations of the spleen, which is both the largest immune organ and one of the sites of highest AuNP accumulation.

In the spleen, arteries enter the red pulp--a framework of collagen and reticular fibers containing fibroblasts, macrophages, and reticular cells-- and branch into smaller arterioles.[19, 20] The blood progresses into the venous sinuses, and most of it passes through the white pulp, which consists of the periarteriolar lymphoid sheath (PALS), the marginal zone, and the follicles. The PALS, also known as the T-cell zone, surrounds the arterioles and is composed of T lymphocytes that interact with dendritic cells and migrating B cells. The follicles are mainly composed of B cells but also contain follicular dendritic cells and T cells. Finally, the marginal zone is an efficient area of blood borne particulate capture, where marginal zone macrophages, dendritic cells, and B cells can act as antigen presenting cells (APCs) and migrate into the follicles to interact with T cells.[19, 20]

Characterizing the distribution of AuNPs within the spleen is valuable for understanding nanoparticle immune effects and for developing nanoparticle mediated immunotherapies. For instance, Yen and colleagues have shown that AuNPs in the 2 nm to 40 nm size range can induce macrophage expression of inflammatory genes for TNFα and IL-6 *in vitro*.[21] Sumbayev et al., in turn, show that AuNPs can suppress IL-1β dependent inflammatory responses *in vitro* and *in vivo* in a size dependent manner.[22] Finally, Tsai and colleagues have demonstrated that treatment with particles in the 4 to 45 nm range can inhibit macrophage toll like receptor 9 responses to CpG, with smaller particles having a stronger effect than larger particles.[23] AuNP mediated therapies have progressed into clinical trials,[24] and thus it is important to further understand AuNP interactions within the immune

system. On the other hand, nanoparticle uptake by immune cells could be exploited in the development of immunotherapies,[25, 26] again illustrating the importance of characterizing such interactions. Here, we assessed the splenic distribution of gold nanoparticles in naïve and tumor bearing mice and showed that AuNPs distributed widely across splenic immune cells, including B cells, T cells, granulocytes, dendritic cells, myeloid derived suppressor cells, and macrophages.

2. Results and Discussion

2.1 Gold nanoparticle characterization

50 nm gold nanoparticles coated with polyethylene glycol (PEG) were chosen as a design representative of particles that would be typically used in cancer applications. The size, shape, and surface coating can be optimized to prolong nanoparticle circulation so that the nanoparticles can reach the target tumor site.[13, 14, 27] Hydrophilic methylated polyethylene glycol (mPEG) coating protects particles from opsonization and subsequent blood clearance, and Perrault and colleagues have shown that PEGylated particles with core sizes in the 20 to 50 nm range are optimal for increased blood half-life.[28] Additionally, it has been shown that 50 nm is the optimal size for mammalian cell uptake of AuNPs.[29] Finally, particles in this size range have been used in a number of applications including photothermal therapy,[30] siRNA delivery,[31] vaccine delivery,[31] and drug delivery.[32]

Therefore, 50 nm gold colloid nanoparticles conjugated with Cy5-terminated PEG-SH (5,000 MW) were used for our studies. Conjugation of the PEG on the gold surface was confirmed by observing a shift in absorbance when compared to the absorbance of citrate stabilized 50 nm gold colloids (Supplementary Figure 1). The spectrum and the red color of the solution also indicated that the particles did not aggregate. The hydrodynamic diameter and zeta potential of the Cy5-PEGylated particles were also comparable to that of normal mPEG coated AuNPs, thus indicating that incorporating Cy5 onto PEG-AuNPs did not alter the particle characteristics (Supplementary Table 1). The PEG coating increased the diameter of the particle by ~ 30 nm compared to the citrate stabilized AuNPs.

2.2 Particle injection does not alter splenic cell distribution

Naïve C57BL/6J mice were injected with approximately 1.5×10^{11} particles in PBS, a dose in the range of previous studies.[33–37] Mice that did not receive particle injections were used as controls. After 1, 6, and 24 hours, the spleens were harvested and stained for the following immune cell populations and markers: $CD3^+$ (T cells), $B220^+$ (B cells), $CD11b^+$ (monocytes and macrophages), $CD11b^+$, $Gr\text{-}1^+$ (myeloid derived suppressor cells), $Gr\text{-}1^+$ (granulocytes), and $CD11c^+$ (dendritic cells). Although there is widespread expression of CD21 and CD23 markers, $CD21^{++}CD23^-$ populations are indicative of marginal zone B cells while $CD21^+CD23^+$ populations are indicative of follicular B cells (Table 1).[38–40] The spleen is mainly composed of $CD3^+$ T cells and $B220^+$ B cells (Figure 1). The myeloid populations of $CD11b^+$ monocytes and macrophages, $CD11b^+Gr\text{-}1^+$ myeloid-derived suppressor cells (MDSCs), $Gr\text{-}1^+$ granulocytes, and $CD11c^+$ dendritic cells each comprise less than 10% of splenocytes. We also noted that the nanoparticle injections caused no

significant differences in the percentages of each population when compared to untreated controls.

2.3 Particles travel from the red pulp to the white pulp of the spleen over time

Histological samples of the spleen were stained with hematoxolin and eosin, and the gold nanoparticles were visualized by dark field microscopy, while their location was correlated with bright field microscopy of the tissue (Figure 2). Untreated spleens displayed only normal tissue scattering and none of the characteristic scattering from nanoparticles. At 1 hour post-injection, the particles appeared and localized mainly within the red pulp and marginal zone of the spleen (red circles) (Figure 2B). At 6 hours, the particles were still present in the marginal zone and red pulp, but they were also visible within the follicles (red arrows) (Figure 2C). Finally, at 24 hours, the particles were mainly located at the center of the follicles while remaining particles were still visible in the red pulp and marginal zone (Figure 2D). These observations indicated that most of the particles moved from the red pulp to the marginal zone and to the middle of the follicle, and were consistent with previous findings by Shah and colleagues.[17] To further ensure that the presence of Cy5 does not affect the distribution of the particles, this experiment was repeated with AuNPs coated with unlabeled mPEG (Supplementary Figure 1). The particles showed the same pattern over time, with most of the particles appearing in the red pulp at 1 hour and progressing to the follicles by 24 hours. Therefore, the presence of Cy5 had negligible effect on the distribution.

2.4 Nanoparticle signal is widely distributed but mainly detected in B cells

To identify the Cy5 positive cells in mice that received nanoparticle injections, gates for Cy5 events were established in untreated mice. The percentage of marker$^+$Cy5$^+$ in the spleen (e.g., B220$^+$Cy5$^+$ divided by all events) was compared between treated and untreated mice for the immune populations mentioned in Table 1 and at all time points (Supplementary Figure 2). All percentages were significantly different than control ($p < 0.01$), showing that the Cy5$^+$ events were from the injected nanoparticles.

Next, we evaluated the distribution of Cy5 events within the immune cells, i.e. the percent of the nanoparticle dose that is in each immune population. For instance, the percent of dose detected within B220$^+$ cells is given by B220$^+$Cy5$^+$ events divided by all Cy5$^+$ events. The distribution of the nanoparticle Cy5 dose in the respective populations at 1, 6, and 24 hours post-injection are shown in Figure 3. At 1 hour, the highest percent of Cy5 events was found within B220$^+$ B cells (32%), and this percentage is significantly higher than that found in CD3$^+$ T cells (12%, $p < 0.0001$), CD11b$^+$ monocytes and macrophages (7.7%, $p < 0.0001$), Gr-1$^+$ granulocytes (15.8%, $p < 0.0001$), CD11c$^+$ dendritic cells (13.6%, $p<0.0001$), CD11b$^+$Gr-1$^+$ MDSCs (3%, $p < 0.0001$), and CD21^{++}CD23$^-$ cells (22.8%, $p < 0.0001$). This finding indicates that the nanoparticles were detected mainly in B cells 1 hour after injection. A detectable percentage of the events (13.6%) was present in dendritic cells despite the low percentage of CD11c$^+$ cells in the spleen. A measureable percentage was also found in other low percentage populations such as Gr-1$^+$ granulocytes and CD11b$^+$Gr-1$^+$ MDSCs, with 15.8% and 3% of the signal detected within these populations, respectively.

At 6 hours, 58.5% of the Cy5 signal was detected in $B220^+$ cells, and the percentage within this population was significantly higher than that found in all other populations ($p < 0.0276$) (Figure 3B). The trend was similar at 24 hours with the highest percentages of Cy5 dose found within $B220^+CD21^{++}CD23^-$, $CD21^+CD23^+$, and $CD11c^+$ cells (Figure 3C). Interestingly, the percentage in B cells increased significantly from 1 hour to 6 hours, going from 32% to 58.5% ($p = 0.0372$) (Figure 3D). The percentage was then significantly decreased at 24 hours to 31.4% ($p = 0.0415$). In turn, the dose in $Gr\text{-}1^+$ cells significantly decreased from 15.8% at 1 hour to 7.3% at 6 hours. The only other change over time was observed in $CD21^+CD23^+$ cells, where the percentage dropped from 36.6% at 6 hours to 17.7% at 24 hours ($p=0.0065$). The cause of these changes was not evident and may be the result of fluorescence differences over time or experimental variability.

There were no other significant differences in Cy5 distribution within each population, and more importantly, the pattern of distribution remained the same across the different time points. The histology images showed that the particles traveled through the spleen over time, and given that the distribution pattern did not change in the 24 hour period, the particles were likely to have migrated with the cells instead of transferring from one cell population to another. The movement of the particles may result from cells such as marginal zone B cells and dendritic cells taking up nanoparticles and then migrating to the follicle.[20] Of course, mechanisms of cellular transfer such as trogocytosis[41] and exocytosis could also be at play, and these potential mechanisms merit further study. The presence of nanoparticles within the marginal zone is consistent with their association with MDSCs, as MDSCs have been shown to be localized within the marginal zone.[42] The markers used here are not exclusive to one population, and there may be overlap within subsets of dendritic cells, B cells, and other immune populations, but the results illustrate that the nanoparticles were distributed across a range of major immune cells including $CD3^+$ T cells, $B220^+$ B cells, $CD11c^+$ dendritic cells, $CD11b^+$ monocytes and macrophages, $CD11b^+Gr\text{-}1^+$ MDSCs, and $Gr\text{-}1^+$ granulocytes. $Cy5^+$ signal within $CD21^{++}CD23^-$ cells may indicate involvement of marginal zone B cells while $CD21^+CD23^+$ cells may indicate follicular B cells;[38, 39] however, uptake by these subsets needs to be further explored in future studies.

Various biodistribution studies have shown that despite AuNP modifications aimed at avoiding spleen and liver uptake, such as PEG coating, targeting ligands, and size and charge variations, a substantial portion of the injected dose will inevitably be retained in the spleen.[13] Studies show a wide range of spleen accumulation, with reports varying between 10% to over 60% of the injected dose reaching the spleen.[27, 34, 43] The consequences of such accumulation are still unclear. A previous study in rats by Tsyntsyuk and colleagues has shown that 50 nm PEGylated gold nanoparticles can cause blood congestion in the red pulp and damage to the white pulp.[44] Balasubramanian et al. studied AuNP effects on gene expression in rat spleens and reported down-regulation of genes associated with healing and other defense responses.[36] Furthermore, as aforementioned, there is ongoing study into the effects of AuNPs on inflammatory responses *in vitro* and *in vivo*.[21-23] In this study, the histology slides were reviewed by an independent pathologist, and the analysis showed that nanoparticle treatment caused no inflammation or signs of splenotoxicity such as apoptosis or atrophy. However, the particle treatment resulted in vascular congestion as well as red pulp expansion, indicated by an increased presence of histiocytes, lymphocytes, and

megakaryocytes. The results presented here elucidate which splenic immune populations interact with nanoparticles after intravenous injection as well as how the spleen reacts to a typically used nanoparticle design and thus can be used to inform future studies on AuNP immune effects.

2.5 Percent of each immune population positive for Cy5 signal

Next, we examined the percentage of each cell population that was Cy5 positive (Figure 4). At 1 hour post injection, approximately 2.9% of $CD21^{++}CD23^{-}$ cells were positive for Cy5, significantly higher than the percentages within all other populations ($p < 0.0086$). This higher proportion as well as the localization of nanoparticles in the marginal zone (Figure 2) again suggests that the particles are taken up by marginal zone B cells. The involvement of marginal zone B cells is likely for this population in mice can uptake blood borne particulates that have been coated with opsonins.[40] AuNPs are known to be opsonized once entering the blood stream[13, 14] and may thus be recognized by marginal zone B cells in the spleen.

By 24 hours, about 2.5% of $CD11c^{+}$ dendritic cells, 3.1% of $Gr\text{-}1^{+}$ granulocytes, and 1.4% of MDSCs were positive for Cy5. Interestingly, these percentages were comparable to the percentage of $B220^{+}$ B cells positive for Cy5, even though the percentage of B cells in the spleen is significantly higher. There were no significant differences in the percentages of cells associated with Cy5 over time, again suggesting that the nanoparticles did not transfer from one cell population to another but instead remained within respective populations that migrate over time. Overall, the distribution of the nanoparticle dose and the percentage of each cell population involved indicate that nanoparticles primarily interact with B cells, T cells, granulocytes, and dendritic cells in the spleen. Importantly, a measureable percentage of the nanoparticle Cy5 signal is detected within MDSCs. Given the comparable percentage of cells positive for Cy5 between myeloid cells and $B220^{+}$ B cells, the myeloid populations may be more efficient at capturing nanoparticles and could potentially be targets for nanoparticle mediated drug delivery.

2.6 Nanoparticle distribution is unaffected in a B16F10 melanoma model

To assess whether these distribution patterns would be the same in a disease model, we tested the nanoparticles in mice bearing a B16F10 melanoma tumor. C57BL/6 mice were implanted with subcutaneous B16F10 tumors and injected with the same dose of particles once the tumors reached approximately 1 cm^3 in size. The spleens were harvested after 24 hours and analyzed as before. The distribution of splenic populations showed a significant drop in $CD3^{+}$ T cells when compared to non-tumor bearing mice ($p = 0.0324$) (Figure 5A). Interestingly, there was no significant difference in either Cy5 events distribution or the percent of cells positive for Cy5 when compared to naïve mice examined 24 hours after nanoparticle injection (Figures 5B and 5C). Therefore, the nanoparticle distribution within major immune cells does not change in tumor bearing mice.

It is worth noting that approximately 22% of Cy5 events were found in $CD11c^{+}$ dendritic cells, with 15% in $Gr\text{-}1^{+}$ granulocytes and 4.8% in $CD11b^{+}Gr\text{-}1^{+}$ MDSCs of tumor bearing mice. Importantly, the nanoparticles reach these populations by passive targeting, without

the aid of ligands or antibodies specific for these cells. The involvement of these populations indicates that they could be potential targets for nanoparticle mediated immunotherapy. The particles' high association with dendritic cells makes them promising vehicles for delivery of immune antigens and adjuvants.[10, 25] In addition, Niikura and colleagues recently reported that 40 nm spherical AuNPs can act as adjuvants for vaccines, for they can induce antigen specific antibody production *in vivo* and bone marrow derived dendritic cell inflammatory responses *in vitro*.[11] The involvement of granulocytes and myeloid derived suppressor cells is also important because granulocytic and myeloid progenitor populations in the spleen have been shown to provide cancer sites with tumor associated macrophages and neutrophils that promote tumor growth.[45] In addition, it has been well established that MDSCs are recruited to the tumor microenvironment and suppress anti-tumor immune responses by inhibiting T cell activity and promoting antigen tolerance.[42, 46] Targeting MDSCs for immune modulation is a promising immune therapy approach that is a subject of ongoing work.[47, 48] Given the association of MDSCs with nanoparticle signal, this population could potentially be targeted with AuNP mediated delivery of drugs that have been shown to suppress MDSC activity, such as sunitinib[49] or CpG.[48, 50]

We also assessed particle distribution in the immune cells of the tumor microenvironment, characterizing Cy5 events within $CD8^+$ cytotoxic T cells, $CD4^+$ helper T cells, $CD11c^+$ dendritic cells, $CD11b^+$ monocytes and macrophages, and $CD11b^+Gr\text{-}1^+$ MDSCs. To ensure that Cy5 events were accurately captured, the percent of $Marker^+Cy5^+$ cells in the entire tumor was calculated in untreated mice and in mice treated with AuNPs, as was done in the spleen. The percentage of $CD11c^+Cy5^+$ cells was significantly higher than in untreated controls ($p=0.0376$), indicating that the Cy5 events were due to the particle injection (Figure 6). This difference was not significant in the other immune populations, and, as such, we could only detect the nanoparticle Cy5 signal within $CD11c^+$ dendritic cells. Approximately 1.8% of the tumor microenvironment was composed of $CD11c^+$ dendritic cells, and about 0.01% of all cells in the microenvironment were $CD11c^+Cy5^+$. However, 36 +/− 10% of all Cy5 events detected were found within $CD11c^+$ cells, indicating that a large portion of the AuNP dose that reaches the tumor resides within dendritic cells. Additionally, 0.7 +/− 0.2% of $CD11c^+$ cells were positive for Cy5. We could not account for the remaining Cy5 signal, but the tumor microenvironment is a complex milieu of inflammatory cells, fibroblasts, blood vessels, and tumor cells,[51, 52] and the distribution of AuNPs within the various cell types merits further work. Overall, nanoparticles reach dendritic cells both in the spleen and the tumor, again illustrating their potential for targeting this population.

3. Conclusions

This study elucidates the immune cell distribution of 50 nm PEG coated gold nanoparticles in the spleen, showing that the nanoparticles associate with a range of immune populations. The signal from the particles is most highly present in B cells, granulocytes, dendritic cells, and T cells, and it appears that the signal remains associated with these populations in the 1 hour to 24 hour range examined in this study. The particles show high association with $CD21^{++}CD23^-$ cells, indicating uptake by marginal zone B cells, but these observations need to be further explored. The anatomical location of the particles vary with time, with AuNPs mainly localizing to the red pulp and marginal zone at 1 hour and appearing in the

marginal zone and follicle between 6 and 24 hours after injection. The consistent particle distribution over time observed using flow cytometry suggests that the particles may migrate with the immune cells as they traverse the spleen. It is possible that marginal zone B cells and dendritic cells take up particles and migrate into the follicle following uptake. Finally, the distribution patterns observed did not vary between tumor bearing and non-tumor bearing mice, and a detectable percentage of Cy5 signal was present in dendritic cells, granulocytes, and MDSCs of the spleens of tumor bearing mice. In addition, AuNPs can be detected in the dendritic cells of the tumor microenvironment. These populations and others could potentially be targeted for cancer immunotherapy, and the distribution characterized here could prove informative for future nanoparticle toxicity studies.

4. Experimental Section

Nanoparticle conjugation

50 nm citrate stabilized gold nanoparticles (Ted Pella) were conjugated with 5,000 MW polyethylene glycol terminated with Cy5 purchased from NanoCS, MA. Absorbance was measured using the Cary 60 UV-Vis (Agilent Technologies), hydrodynamic diameter was measured using a 90 Plus Particle Size Analyzer (Brookhaven), and the zeta potential was measured with a Zen 3600 Zetasizer (Malvern Instruments).

Animal studies and tumor model

C57BL/6J mice (Jackson Laboratories, Bar Harbor, ME) were kept in the Animal Resource Facility of Rice University, and the study was approved by the Institutional Animal Care and Use Committee. The particles were suspended in PBS and injected intravenously at a concentration of 1.5×10^{11} particles per injection. After 1 (n=6), 6 (n=6), or 24 hours (n=5), the mice were euthanized, and the spleens were harvested by passing through a 70 μm cell strainer. The cell suspension underwent red blood cell lysis (Sigma) prior to staining with antibodies. The following antibodies were obtained from BD Biosciences and used for flow cytometry analysis: anti-CD11c PE, anti-B220 PE, anti-CD3 FITC, anti-CD11b PE, anti-Gr-1 FITC, anti-CD23 PE, and anti-CD21 FITC. The stained samples were then analyzed using a BD FACSCanto I flow cytometer.

For the tumor study, mice were injected subcutaneously with 5×10^{5} B16-F10 melanoma cells in PBS (n=7). Once the tumors reached approximately 1 cm^2 in size, the mice received an intravenous injection of nanoparticles. Tumor bearing mice that did not receive particle injections were used as controls (n=4). The spleens were harvested after 24 hours and analyzed as previously described. The tumors were also harvested, passed through a cell strainer, and treated with red blood cell lysis buffer. The following antibodies were used for flow cytometry: anti-CD8 PE, anti-CD3 FITC, anti-CD11c PE, anti-CD11b PE, and anti-GR-1 FITC (BD Biosciences). The B16F10 cells were grown in Dulbecco's Modified Eagle Medium (DMEM), supplemented with 10% Fetal Bovine Serum (FBS) and 1% penicillin/streptomycin. The cells were kept at 37 °C and 5% CO_2.

Histological images

Spleen tissue was formalin fixed and dehydrated in ethanol prior to sectioning. The sections were prepared as 3 μm paraffin-embedded slides stained with hematoxylin and eosin (H&E) at the Baylor College of Medicine Pathology Core. Brightfield images were taken with a Zeiss Axioskop 2 Plus microscope, and darkfield images were taken with a Cytoviva enhanced darkfield microscope.

Statistics

All comparisons were done using a significance level of $\alpha=0.05$, and the Tukey's HSD test on JMP Pro Software.

Supplementary Material

Refer to Web version on PubMed Central for supplementary material.

Acknowledgments

This project was funded by supported by the National Institutes of Health R01CA172836. This research was also funded by a training fellowship from the Keck Center of the Gulf Coast Consortia, on the Nanobiology Interdisciplinary Graduate Training Program, National Institute of Biomedical Imaging and Bioengineering (NIBIB) T32EB009379. J. Almeida also received support from the National Science Foundation Graduate Research Fellowship #0940902 and the Howard Hughes Medical Institute Med into Grad fellowship. A. Lin received support from the Medical Scientist Training Program at Baylor College of Medicine, the Edward and Josephine Hudson Scholarship, and the Ruth L. Kirschstein National Research Service Awards for Individual Predoctoral MD/PhD Fellows (F30) by NIH and NCI.

References

1. Kennedy LC, Bickford LR, Lewinski NA, Coughlin AJ, Hu Y, Day ES, West JL, Drezek RA. Small. 2011; 7:169. [PubMed: 21213377]
2. Han G, Ghosh P, Rotello VM. Nanomedicine. 2007; 2:113. [PubMed: 17716197]
3. Paciotti GF, Myer L, Weinreich D, Goia D, Pavel N, McLaughlin RE, Tamarkin L. Drug Delivery. 2004; 11:169. [PubMed: 15204626]
4. Qiao G, Zhuo L, Gao Y, Yu L, Li N, Tang B. Chemical Communications. 2011, 47:7458. [PubMed: 21589964]
5. Cho WS, Cho MJ, Jeong J, Choi M, Cho HY, Han BS, Kim SH, Kim HO, Lim YT, Chung BH. Toxicology and Applied Pharmacology. 2009; 236:16. [PubMed: 19162059]
6. Loo C, Lowery A, Halas NJ, West J, Drezek R. Nano Letters. 2005; 5:709. [PubMed: 15826113]
7. Hurst SJ, Lytton-Jean AKR, Mirkin CA. Analytical Chemistry. 2006; 78:8313. [PubMed: 17165821]
8. Lee IH, Kwon HK, An S, Kim D, Kim S, Yu MK, Lee JH, Lee TS, Im SH, Jon S. Angewandte Chemie - International Edition. 2012; 51:8800.
9. Wei M, Chen N, Li J, Yin M, Liang L, He Y, Song H, Fan C, Huang Q. Angewandte Chemie - International Edition. 2012; 51:1202
10. Lin AY, Lunsford J, Bear AS, Young JK, Eckels P, Luo L, Foster AE, Drezek RA. Nanoscale Research Letters. 2013; 8:1. [PubMed: 23279756]
11. Niikura K, Matsunaga T, Suzuki T, Kobayashi S, Yamaguchi H, Orba Y, Kawaguchi A, Hasegawa H, Kajino K, Ninomiya T, Ijiro K, Sawa H. ACS Nano. 2013
12. Lin AY, Mattos Almeida JP, Bear A, Liu N, Luo L, Foster AE, Drezek RA. PLoS ONE. 2013; 8:e63550. [PubMed: 23691064]
13. Almeida JPM, Chen AL, Foster A, Drezek R. Nanomedicine. 2011; 6:815. [PubMed: 21793674]
14. Khlebtsov N, Dykman L. Chemical Society Reviews. 2011

15. Alkilany AM, Murphy CJ. Journal of Nanoparticle Research. 2010; 12:2313. [PubMed: 21170131]
16. Hirn S, Semmler-Behnke M, Schleh C, Wenk A, Lipka J, Schäffler M, Takenaka S, Möller W, Schmid G, Simon U, Kreyling WG. European Journal of Pharmaceutics and Biopharmaceutics. 2011; 77:407. [PubMed: 21295759]
17. Shah DB, Vercellotti GM, White JG, Fegan A, Wagner CR, Bischof JC. Molecular Pharmaceutics. 2012; 9:2146. [PubMed: 22668197]
18. Bartneck M, Ritz T, Keul HA, Wambach M, Bornemann J, Gbureck U, Ehling J, Lammers T, Heymann F, Gassler N, Ludde T, Trautwein C, Groll J, Tacke F. ACS Nano. 2012; 6:8767. [PubMed: 22994679]
19. Gesta MF. Toxicologic Pathology. 2006; 34:455. [PubMed: 17067939]
20. Mebius RE, Kraal G. Nature Reviews Immunology. 2005; 5:606.
21. Yen HJ, Hsu SH, Tsai CL. Small. 2009; 5:1553. [PubMed: 19326357]
22. Sumbayev VV, Yasinska IM, Garcia CP, Gilliland D, Lall GS, Gibbs BF, Bonsall DR, Varani L, Rossi F, Calzolai L. Small. 2013; 9:472. [PubMed: 23112137]
23. Tsai CY, Lu SL, Hu CW, Yeh CS, Lee GB, Lei HY. Journal of Immunology. 2012; 188:68.
24. Libutti SK, Paciotti GF, Byrnes AA, Alexander Jr HR, Gannon WE, Walker M, Seidel GD, Yuldasheva N, Tamarkin L. Clinical Cancer Research. 2010; 16:6139. [PubMed: 20876255]
25. Moon JJ, Huang B, Irvine DJ. Advanced Materials. 2012; 24:3724. [PubMed: 22641380]
26. Borsacchi D, Costantino L, Italiani P. Nanomedicine. 2012; 7:121. [PubMed: 22191781]
27. Zhang GD, Yang Z, Lu W, Zhang R, Huang Q, Tian M, Li L, Liang D, Li C. Biomaterials. 2009; 30:1928. [PubMed: 19131103]
28. Perrault SD, Walkey C, Jennings T, Fischer HC, Chan WCW. Nano Letters. 2009; 9:1909. [PubMed: 19344179]
29. Chithrani BD, Ghazani AA, Chan WCW. Nano Letters. 2006; 6:662. [PubMed: 16608261]
30. Bear AS, Kennedy LC, Young JK, Perna SK, Mattos Almeida JP, Lin AY, Eckels PC, Drezek RA, Foster AE. PLoS ONE. 2013; 8:e69073. [PubMed: 23935927]
31. Lu W, Zhang G, Zhang R, Flores II LG, Huang Q, Gelovani JG, Li C. Cancer Research. 2010; 70:3177. [PubMed: 20388791]
32. You J, Zhang R, Zhang G, Zhong M, Liu Y, Van Pelt CS, Liang D, Wei W, Sood AK, Li C. Journal of Controlled Release. 2012; 158:319. [PubMed: 22063003]
33. Sonavane G, Tomoda K, Makino K. Colloids and Surfaces B-Biointerfaces. 2008; 66:274.
34. Kennedy LC, Bear AS, Young JK, Lewinski NA, Kim J, Foster AE, Drezek RA. Nanoscale Research Letters. 2011; 6:X1.
35. Hirsch LR, Stafford RJ, Bankson JA, Sershen SR, Rivera B, Price RE, Hazle JD, Halas NJ, West JL. Proceedings of the National Academy of Sciences of the United States of America. 2003; 100:13549. [PubMed: 14597019]
36. Balasubramanian SK, Jittiwat J, Manikandan J, Ong CN, Yu LE, Ong WY. Biomaterials. 2010; 31:2034. [PubMed: 20044133]
37. Day ES, Thompson PA, Zhang L, Lewinski NA, Ahmed N, Drezek RA, Blaney SM, West JL. Journal of Neuro-Oncology. 2011; 104:55. [PubMed: 21110217]
38. Pillai S, Cariappa A, Moran ST. Marginal zone B cells. 2005; Vol. 23:161.
39. Pillai S, Cariappa A. Nature Reviews Immunology. 2009; 9:767.
40. Cerutti A, Cols M, Puga I. Nature Reviews Immunology. 2013; 13:118.
41. Ahmed KA, Munegowda MA, Xie Y, Xiang J. Cellular and Molecular Immunology. 2008; 5:261. [PubMed: 18761813]
42. Ugel S, Peranzoni E, Desantis G, Chioda M, Walter S, Weinschenk T, Ochando JC, Cabrelle A, Mandruzzato S, Bronte V. Cell Reports. 2012; 2:628. [PubMed: 22959433]
43. Lipka J, Semmler-Behnke M, Sperling RA, Wenk A, Takenaka S, Schleh C, Kissel T, Parak WJ, Kreyling WG. Biomaterials. 2010; 31:6574. [PubMed: 20542560]
44. Terentyuk GS, Maslyakova GN, Suleymanova LV, Khlebtsov BN, Kogan BY, Akchurin GG, Shantrocha AV, Maksimova IL, Khlebtsov NG, Tuchin VV. Journal of Biophotonics. 2009; 2:292. [PubMed: 19434616]

45. Cortez-Retamozo V, Etzrodt M, Newton A, Rauch PJ, Chudnovskiy A, Berger C, Ryan RJH, Iwamoto Y, Marinelli B, Gorbatov R, Forghani R, Novobrantseva TI, Koteliansky V, Figueiredo JL, Chen JW, Anderson DG, Nahrendorf M, Swirski FK, Weissleder R, Pittet MJ. Proceedings of the National Academy of Sciences of the United States of America. 2012; 109:2491. [PubMed: 22308361]
46. Mundy Bosse BL, Lesinski GB, Jaime-Ramirez AC, Benninger K, Khan M, Kuppusamy P, Guenterberg K, Kondadasula SV, Chaudhury AR, La Perle KM, Kreiner M, Young G, Guttridge DC, Carson Iii WE. Cancer Research. 2011; 71:5101. [PubMed: 21680779]
47. Kao J, Ko EC, Eisenstein S, Sikora AG, Fu S, Chen SH. Critical Reviews in Oncology/Hematology. 2011; 77:12. [PubMed: 20304669]
48. Shirota Y, Shirota H, Klinman DM. Journal of Immunology. 2012; 188:1592.
49. Ko JS, Zea AH, Rini BI, Ireland JL, Elson P, Cohen P, Golshayan A, Rayman PA, Wood L, Garcia J, Dreicer R, Bukowski R, Finke JH. Clinical Cancer Research. 2009; 15:2148. [PubMed: 19276286]
50. Zoglmeier C, Bauer H, Nörenberg D, Wedekind G, Bittner P, Sandholzer N, Rapp M, Anz D, Endres S, Bourquin C. Clinical Cancer Research. 2011; 17:1765. [PubMed: 21233400]
51. Cuadrillos-Ruiz JR, Rutkowski M, Conejo-Garcia JR. Cell Cycle. 2010; 9:260. [PubMed: 20023378]
52. Whiteside TL. Oncogene. 2008; 27:5904. [PubMed: 18836471]

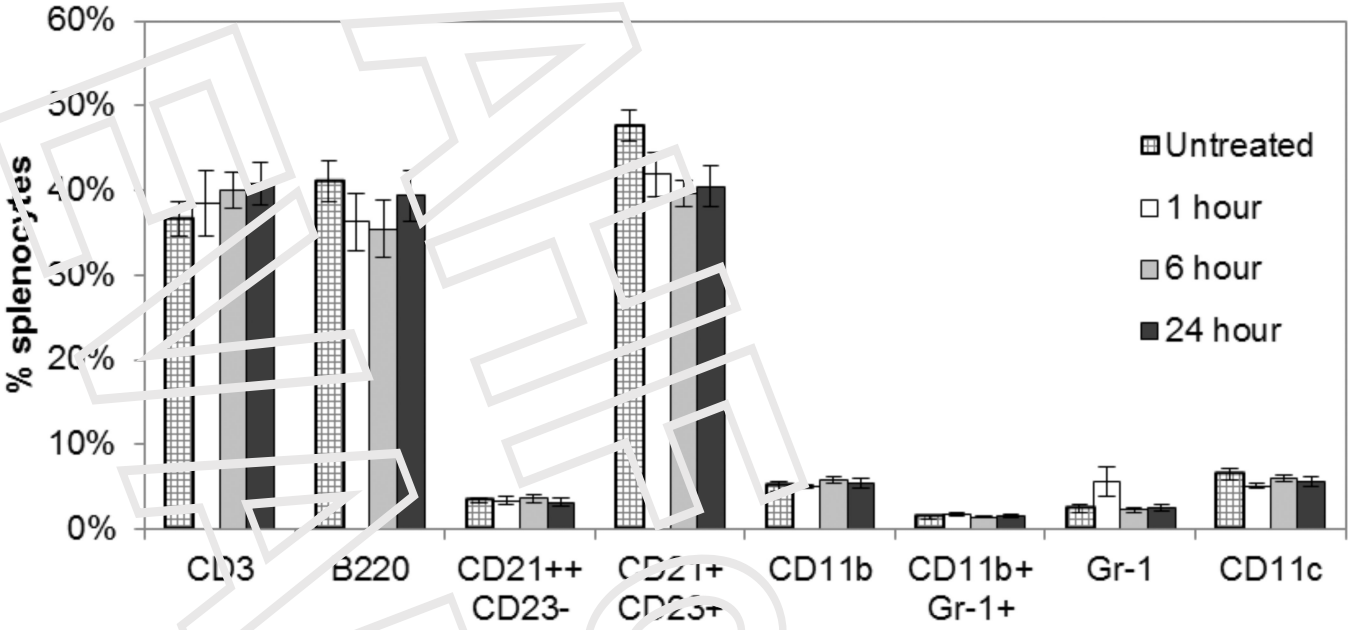

Figure 1

Percentage of immune populations in the spleens of mice that were untreated or harvested 1, 6 or 24 hours after AuNP intravenous injection.

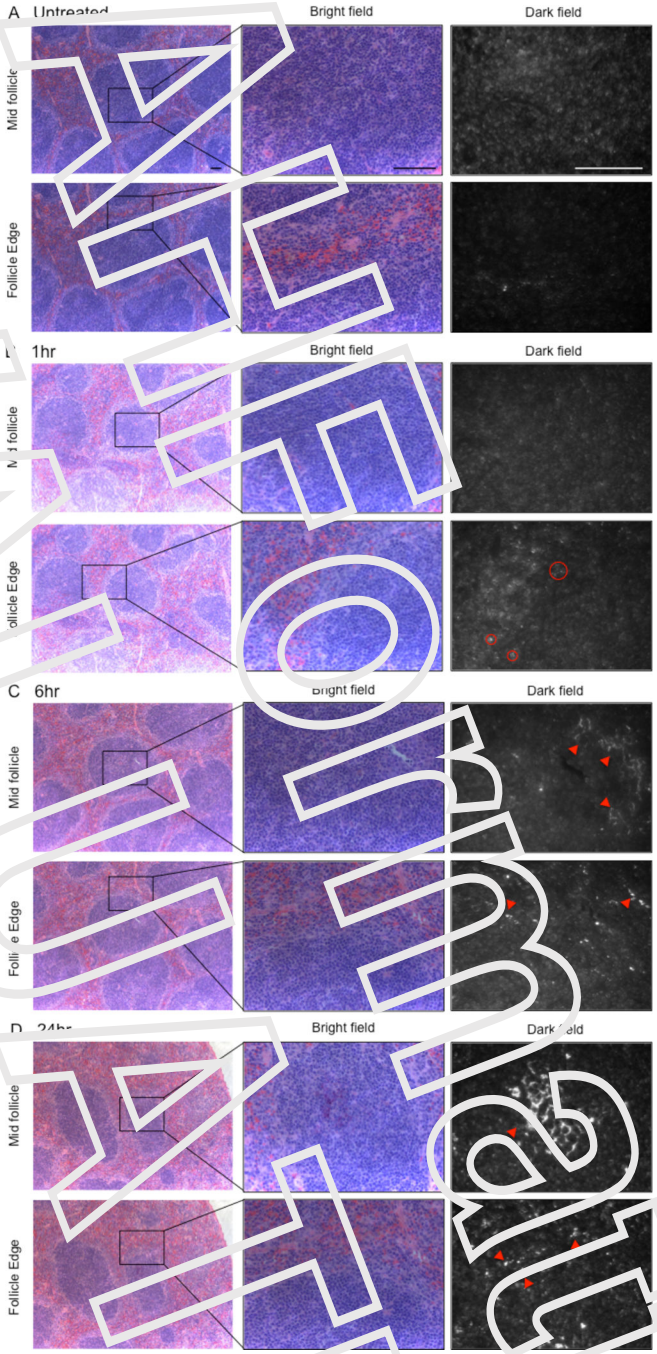

Figure 2.

H&E bright field and dark field images of murine spleens at middle and edges of the follicles. A) Untreated spleen. B) Spleen 1 hour following AuNP injection. C) Spleen 6 hours after AuNP injection. D) Spleen 24 hours after AuNP injection. Images are representative of 3 samples. (Scale bar = 100 μm)

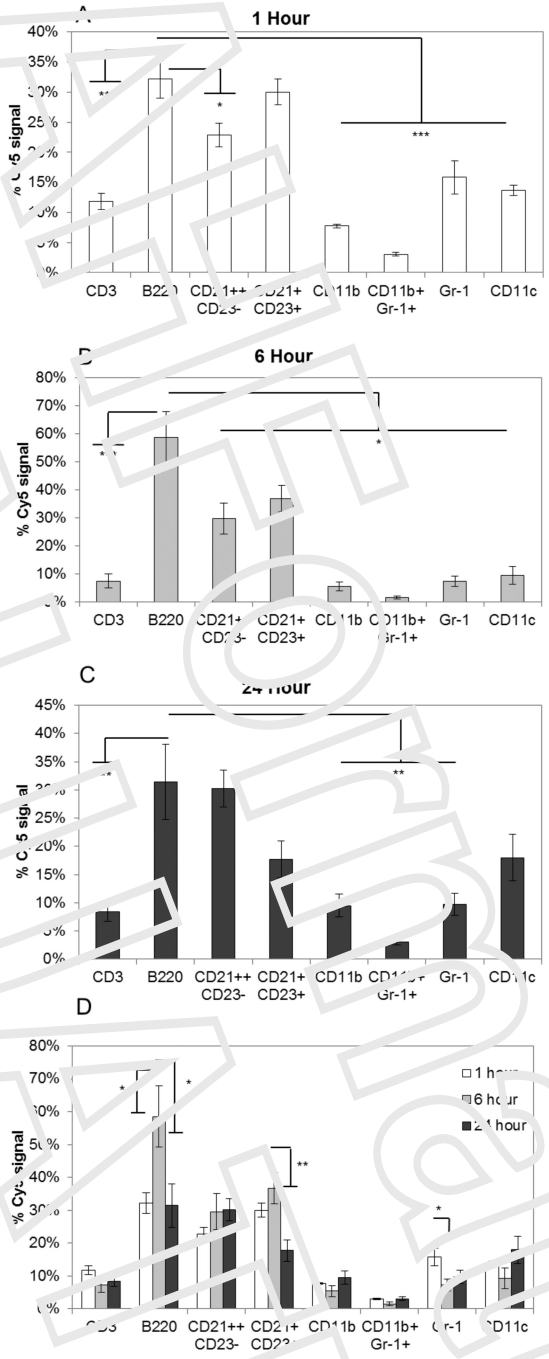

Figure 3.

Distribution of AuNP associated Cy5 positive signal within immune populations at different time points. A) 1 hour, B) 6 hours, and C) 24 hours after AuNP intravenous injection. D) Distribution of Cy5 signal within immune populations at all time points. *, $p<0.05$. **, $p<0.01$. ***, $p<0.0001$.

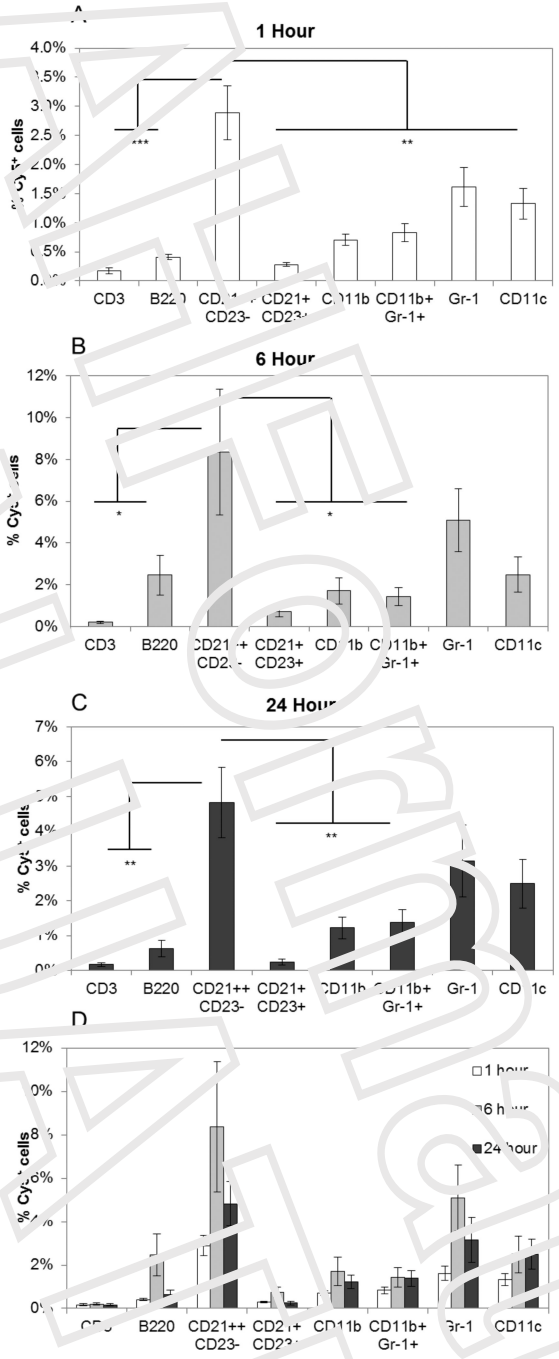

Figure 4.

Percent of each immune population associated with AuNP Cy5 signal A) 1 hour, B) 6 hours, and C) 24 hours after AuNP injection. D) Percent of each immune population associated with AuNP Cy5 signal at all time points. *, $p<0.05$. **, $p<0.01$. ***, $p<0.0001$.

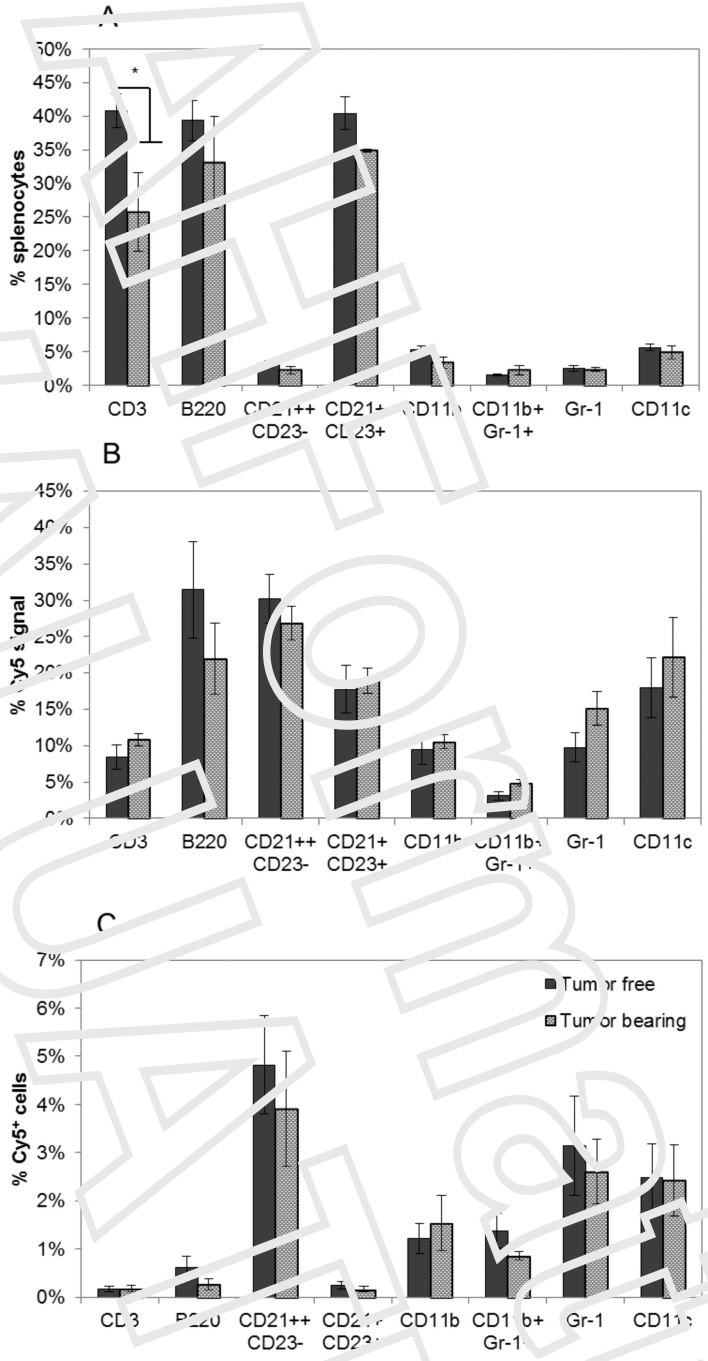

Figure 5.

Comparison of particle distribution in the spleen between tumor free and tumor bearing mice. A) Percent of each immune population in the spleens of tumor free and tumor bearing mice. B) Distribution of Cy5 signal within each immune population 24 hours after AuNP injection in tumor free and tumor bearing mice. C) Percent of each immune population associated with Cy5 signal 24 hours after AuNP injection in tumor free and tumor bearing mice. *, $p<0.05$.

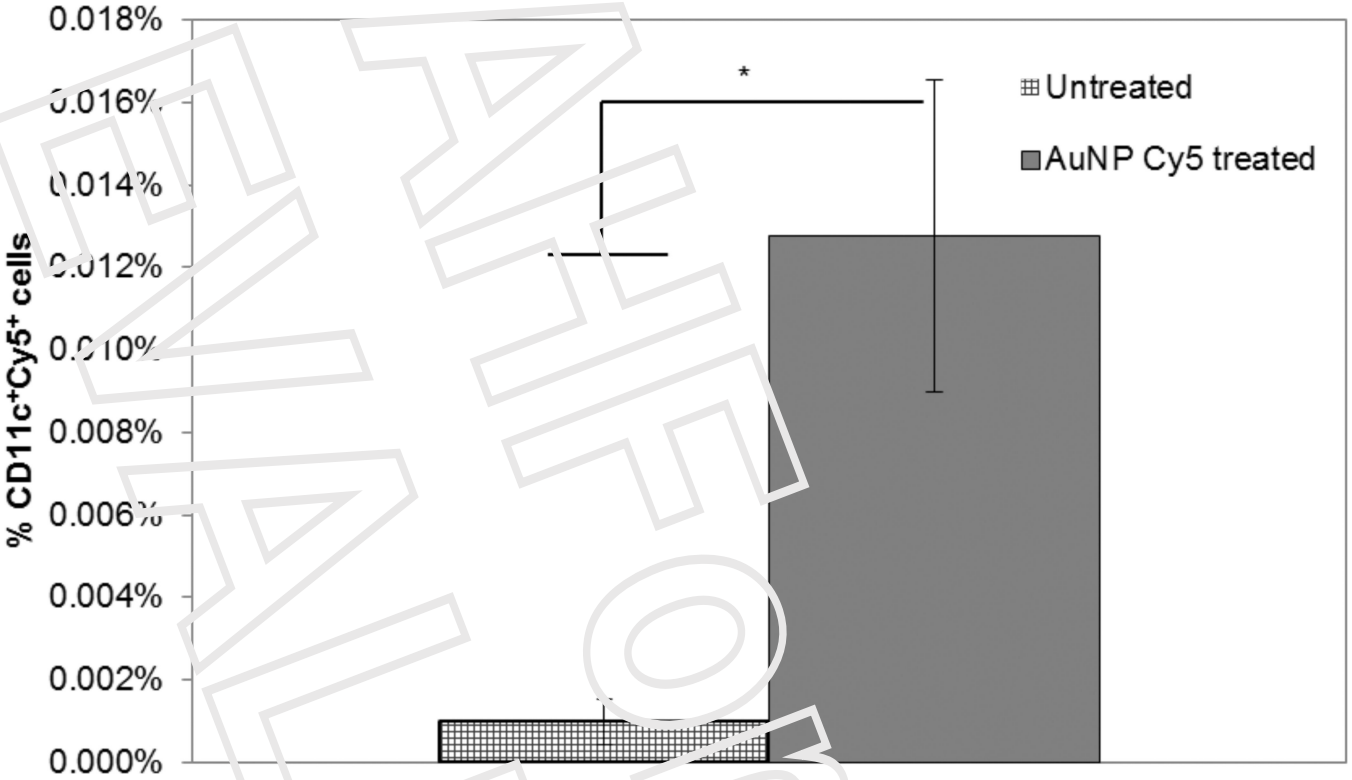

Figure 6

Percentage of CD11c positive and particle positive cells ($CD11c^{+}Cy5^{+}$) in the tumor microenvironment. *, $p < 0.05$.

Table 1

Immune populations analyzed by flow cytometry.

Marker	Immune population
CD3	T cells
B220	B cells
$CD21^{++}CD23^{-}$	Suggestive of marginal zone B cells
$CD21^{+}CD23^{+}$	Suggestive of follicular B cells
CD11b	Monocytes and macrophages
$CD11b^{+}Gr\text{-}1^{+}$	Myeloid-derived suppressor cells
Gr-1	Granulocytes
CD11c	Dendritic cells